Author's personal copy

Microporous and Mesoporous Materials 134 (2010) 22–28

Contents lists available at ScienceDirect

Microporous and Mesoporous Materials

journal homepage: www.elsevier.com/locate/micromeso

NMR study of proton transfer to strong bases on inner surfaces of MCM-41

B.C.K. Ip [a], D.V. Andreeva [a,1], G. Buntkowsky [b], D. Akcakayiran [c], G.H. Findenegg [c], I.G. Shenderovich [a,d,*]

[a] Institut für Chemie und Biochemie, Freie Universität Berlin, Takustrasse 3, 14195 Berlin, Germany
[b] Eduard-Zintl-Institut für Anorganische und Physikalische Chemie, Technische Universität Darmstadt, Petersenstrasse 20, 64287 Darmstadt, Germany
[c] Institut für Chemie, Technische Universität Berlin, Strasse des 17. Juni 124, 10623 Berlin, Germany
[d] Department of Physics, St. Petersburg State University, Ulianovskaya 1, 198504 St. Petersburg, Russian Federation

ARTICLE INFO

Article history:
Received 16 March 2010
Received in revised form 29 April 2010
Accepted 2 May 2010
Available online 6 May 2010

Keywords:
Hydrogen bond
Proton transfer
NMR spectroscopy
MCM-41
Host–guest systems

ABSTRACT

Variable temperature ^{1}H and ^{15}N NMR techniques have been used to study the interaction of ^{15}N enriched 4-dimethylaminopyridine (AP) and 4-diethyl-2,6-di-tert-butylaminopyridine (TBAP) with the surface of MCM-41 silica. Both bases become protonated on the surface. $[AP\text{-}H]^+$ and $[TBAP\text{-}H]^+$ remain immobilized on the surface at room temperature, but are free to rotate around the molecular C_2 axis. The concentration of the protonated species is not affected by the presence of water and water is not involved in or coordinated around the protonated species. We propose that strong electrostatic interactions can affect the local structure of the inner surfaces of MCM-41 that result in mutual interactions of neighboring silanol groups which enables proton transfer to the guests. There are good reasons to suggest that three surface silanol groups are involved in each cluster with one protonated base. The N···H distance in the $[AP\text{-}H]^+$ cation is lengthened by a hydrogen bond to the deprotonated silanol group. The N···H distance in the $[TBAP\text{-}H]^+$ cation is shorter and the interaction to the anion is purely electrostatic. In the presence of water and an excess of AP, 2:1 AP:water complexes are formed, with one water bonded between two bases and the N···H distances of about 1.7 Å. The reorientation of these complexes and the molecular exchange among different species are slow at room temperature. TBAP does not interact with water on the silica surface.

© 2010 Elsevier Inc. All rights reserved.

1. Introduction

Ordered mesoporous silicas, although still too expensive for industrial applications, are regarded to have a high potential as catalytic supports and host materials for organic guest molecules and transition metals [1–8]. These expectations have triggered several studies of the dynamics of guest molecules in these materials [9–12]. One of the central points of these studies was the host–guest interactions at inner silica surfaces. As these interactions are mainly affected by the potential chemical reactivity and the distribution of silanol groups, the properties of these groups were extensively studied in the past [13–15]. These properties depend on the type and the method of preparation of the material studied [16–19]. Some methods used to determine the number of OH-groups at inner surfaces of silica materials have been reviewed in Ref. [20]. Recently, some of us have studied the potential chemical reactivity and the distribution of silanol groups of MCM-41 using NMR spectroscopy. It has been shown that MCM-41 materials calcined at 823 K contains about 2.9 surface silanol groups per nm^2 [21]. The proton-donating ability of these groups under water-free conditions is equivalent to that of acids of $pK_a \approx 5$ [21]. As a result, in the absence of water the pore walls of MCM-41 are relatively inert with regard to chemical reactions with guest molecules. For example, pyridine adsorption leads to N···HOSi hydrogen bonds of the length of about 1.7 Å [21]. However, the structure of acid–base complexes generally depends strongly on their environment [22–25]. For example, the hydrogen bond interaction of pyridine with sulfonic and phosphonic acid moieties at the surfaces of SBA-15 silica has been studied by a combination of solid-state NMR techniques [26]. It has been shown that for both materials, the interaction of the acid moieties with the base results in proton transfer to pyridine. The observed proton-donating ability of the acid moieties was affected by the presence of residual water, since the sulfonic acid-functionalized SBA-15 material contained about six water molecules per acid moiety after drying at 420 K in high vacuum. It was not possible to reduce the amount of the residual water since a drying process at higher temperature would result in thermal decomposition of the functionalized surface. Alternatively, one can control easily the amount of water at the silica

* Corresponding author at: Institut für Chemie und Biochemie, Freie Universität Berlin, Takustrasse 3, 14195 Berlin, Germany. Tel.: +49 (0) 30 83853615; fax: +49 (0) 30 83855310.
E-mail addresses: brendaip@chemie.fu-berlin.de (B.C.K. Ip), daria.andreeva@uni-bayreuth.de (D.V. Andreeva), Gerd.Buntkowsky@chemie.tu-darmstadt.de (G. Buntkowsky), dilek@chem.tu-berlin.de (D. Akcakayiran), findenegg@chem.tu-berlin.de (G.H. Findenegg), shender@chemie.fu-berlin.de (I.G. Shenderovich).
[1] Present address: Phys. Chem. II, Universität Bayreuth, 95440 Bayreuth, Germany.

1387-1811/$ - see front matter © 2010 Elsevier Inc. All rights reserved.
doi:10.1016/j.micromeso.2010.05.003

Author's personal copy

surface, when pure siliceous SBA-15 and MCM-41 silicas are used. Mesoporous silica materials contain some adsorbed water at ambient conditions, which interacts with the silanol groups. At higher loadings, a second and further adsorbed layers and/or bulk-like water in the core of the pore space can be formed [27–29]. On the other hand, evacuation of such materials at 400 K for several hours is sufficient to remove adsorbed water that render water-free silica host materials [21,27].

The goal of the present work is to study the hydrogen bond interaction between the surface silanol groups of pure siliceous MCM-41 and very strong proton acceptors. We expect that the inspection of the properties of host–guest interactions will make it possible to characterize the local morphology of the amorphous silica surface. In particular, it is not clear whether adsorbed water can affect the proton-donor ability of the surface silanol groups. Indeed, the sulfonic and phosphonic acid moieties were attached to silica surface through a long linker and could be solvated by water molecules [26]. In contrast, the silanol groups are attached directly to the surface and thus the situation is different from solvation in solution. We used ^{15}N enriched 4-dimethylaminopyridine (AP) and 4-diethyl-2,6-di-tert-butylaminopyridine (TBAP) as the probe molecules, as the functional dependence of the isotropic ^{15}N NMR chemical shift of pyridines on the hydrogen bond geometry is well-known [30]. Both molecules are potentially very strong proton acceptors and are characterized by the theoretically predicted pK_a values of 9.5 and 11.1 for AP and TBAP, respectively [31]. However, the presence of the tert-butyl groups in the ortho positions affects dramatically the geometry of hydrogen-bonded complexes of TBAP. Although it has been suggested that TBAP can form hydrogen bonds with water in the gas and the aqueous phase [32], its solubility in water is very low. In fact, the only way it can form a hydrogen bond with an acid is to deprotonate the latter [33]. Thus, one expects that the surface silanol groups will be accessible for AP, as they are accessible for pyridine. In contrast, their interaction with TBAP should be strongly hindered. To characterize the interactions between silanol groups and the guests in the presence and absence of adsorbed water, three types of measurements were necessary: (1) inspection of the protonation state of the probe molecules loaded into MCM-41 kept at ambient conditions using ^{15}N MAS NMR, (2) characterization of the protonation state of the probe molecules loaded into MCM-41 evacuated at 420 K overnight using ^{15}N MAS NMR and (3) analysis of the dynamics of the probe molecules on silica surface using ^{1}H MAS NMR.

2. Experimental section

2.1. Materials

The MCM-41 material was synthesized following the procedure of Grün et al. [34] in aqueous ammonia solutions, using C_{16}-trimethylammonium bromide as template and TEOS as the silica precursor. It was the same material as sample M2 of Ref. [42]. Details of the synthesis are given elsewhere [35]. The precipitated product was kept in the reaction solution at 308 K for 24 h and at 373 K again for 24 h. After rinsing with pure water and drying the powder was heated in air first to 453 K for 4 h, to remove most of the polymer template, and finally calcinated at 823 K under air flow.

The porosity of the material was characterized by nitrogen adsorption using the DFT pore size analysis method [36]. A specific surface area $a_{BET} = 1000\ m^2/g$ and specific pore volume $v_p = 0.96\ cm^3/g$ was found, and a pore diameter $D = 3.9$ nm was derived from the pore condensation pressure ($p/p_0 = 0.358$) by the Kruk–Jaroniec–Sayari relation [37]. From the pore diameter and the lattice constant of the 2D hexagonal pore lattice, $a_0 = 4.67$ nm (obtained by small-angle XRD), a pore center-to-center wall thickness $w = a_0 - D = 0.8$ nm was found.

2.1.1. Synthesis of 4-dimethylaminopyridine-^{15}N (AP)

The substance was synthesized following the procedure of Kumar et al. [38], using ^{15}N enriched pyridine. AP with the deuterated methyl groups was synthesized by the same method, using *N*,*N*-dimethylmethanamide (DMF-d_6).

2.1.2. Synthesis of 4-diethyl-2,6-di-tert-butylaminopyridine-^{15}N (TBAP)

The substance was synthesized following the procedure of Potts et al. [39], using aqueous ammonia-^{15}N (25%) in ethanol, yielding 60% of TBAP. The aqueous ammonia-^{15}N solution was prepared

Table 1
Samples of MCM-41 loaded with pyridine derivatives studied in this work.

Sample[a]	Amount in mg		Preparation		Resonances in ^{15}N NMR	Species per nm^2 [f]
	Host[b]	Guest[c]	Host[d]	Solvent[e]		
AP-1	40	6	Ambient	CH_2Cl_2	124	0.7
AP-2	24	16	Ambient	CH_2Cl_2	220	2.6
					124	0.6
AP-3	15	15	Ambient	CH_2Cl_2	236	1.8
					220	2.8
					124	0.3
AP-3w	AP-3 loaded with 1 mg of H_2O					
TBAP-1	60	5	Stored over water	CH_2Cl_2	109	0.2
TBAP-2	40	40	Ambient	CH_2Cl_2	235	2.3
					109	<0.2
TBAP-3	46	21	Ambient	C_6H_{14}	235	0.7
					109	0.3
TBAP-4	45	20	Ambient	CH_3CN	235	0.8
					109	0.2
TBAP-5			Dry	CH_2Cl_2	109	
TBAP-6			Dry	C_6H_{14}	109	

[a] AP stands for samples loaded with ^{15}N enriched 4-dimethylaminopyridine and TBAP stands for samples loaded with ^{15}N enriched 4-diethyl-2,6-di-tert-butylaminopyridine.
[b] MCM-41.
[c] Pyridine derivative.
[d] Ambient stands for samples prepared without pre-drying of MCM-41 and dry stands for samples prepared using MCM-41 evacuated overnight at 420 K in high vacuum.
[e] Solvent used to assist to distribute guest molecules.
[f] Number of molecules per nm^2 of MCM-41.

Author's personal copy

from ^{15}N enriched ammonium chloride in a Clasius retrograding modified gas-development apparatus.

2.1.3. Sample preparation

Specific features of samples used in this study are given in Table 1.

Samples labeled as "ambient" were prepared as follows: MCM-41 kept at ambient conditions was placed into a 5 mm NMR tube equipped with a Young valve. The probe base was dissolved in 1 ml of water-free organic solvent (dichloromethane, *n*-hexane or acetonitrile). This solution was added to the silica in the NMR tube and kept for 12 h to ensure a homogeneous distribution of the probe molecules in the pores. The solvent was then removed slowly *in vacuo* (1 Pa) at room temperature. Samples labeled as "dry" were prepared as follows: the silica material was dried *in vacuo* (10^{-3} Pa) at 420 K for >18 h and transferred into a 5 mm NMR tube equipped with a Young valve under argon atmosphere in a glove bag. The probe base was then added inside the glove bag in the same way as described above.

Sample TBAP-1 was kept in a desiccator over pure water for 1 week.

Sample AP-3w was prepared from AP-3 by adding 1 mg of water and allowing 24 h to ensure a uniform distribution of water.

2.2. NMR measurements

The ^{1}H and ^{15}N NMR measurements were performed on a Bruker MSL-300 instrument operating at 7 Tesla, equipped with a variable-temperature Chemagnetics-Varian 6 mm pencil CPMAS probe. Under MAS conditions the samples were spun at 6 kHz.

2.2.1. ^{1}H NMR measurements

The ^{1}H MAS spectra were recorded employing a 90°-pulse length of 3.5 μs and a recycle delay of 5 s. The number of scans was 64. All ^{1}H chemical shift values are referenced to trimethylsilyl-2,2,3,3-tetradeuteropropionic acid (TSP; sodium salt).

2.2.2. ^{15}N NMR measurements

The $\{^{1}H\}$–^{15}N CPMAS spectra were recorded using a cross-polarization contact time of 5 ms, the typical 90°-pulse lengths were about 4.0 μs, and a recycle delay of 5 s. All ^{15}N chemical shift values are referenced to the solid $^{15}NH_4Cl$ scale.

3. Results

In this section the results of NMR experiments are reported. The interpretation of the obtained results is given in Section 4. Variable temperature ^{15}N NMR was used to inspect the protonation state of the probe molecules accommodated in MCM-41 under different conditions. AP and TBAP in the crystalline state resonate at 236 and 235 ppm, respectively. ^{1}H NMR is used to compare the dynamics of AP and pyridine on the silica surface at room temperature.

3.1. ^{15}N NMR

Fig. 1 presents ^{15}N NMR spectra of MCM-41 loaded with AP. Sample AP-1 contained 0.7 AP molecules per nm^2 of the silica surface. This sample is characterized by a signal at 124 ppm, Fig. 1a–c. The signal-to-noise ratio is the best for the spectrum obtained under the ^{1}H–^{15}N cross-polarization (CP) and MAS condition, Fig. 1a. The spectral line in the static spectrum is broader than the MAS spectrum but isotropic, Fig. 1c. Samples AP-2 and AP-3 contained about 3.2 and 4.9 molecules per nm^2, respectively. Besides the signal at 124 ppm a signal at 220 ppm appears in the ^{15}N CPMAS NMR spectrum of AP-2, Fig. 1d. The same resonances and an additional

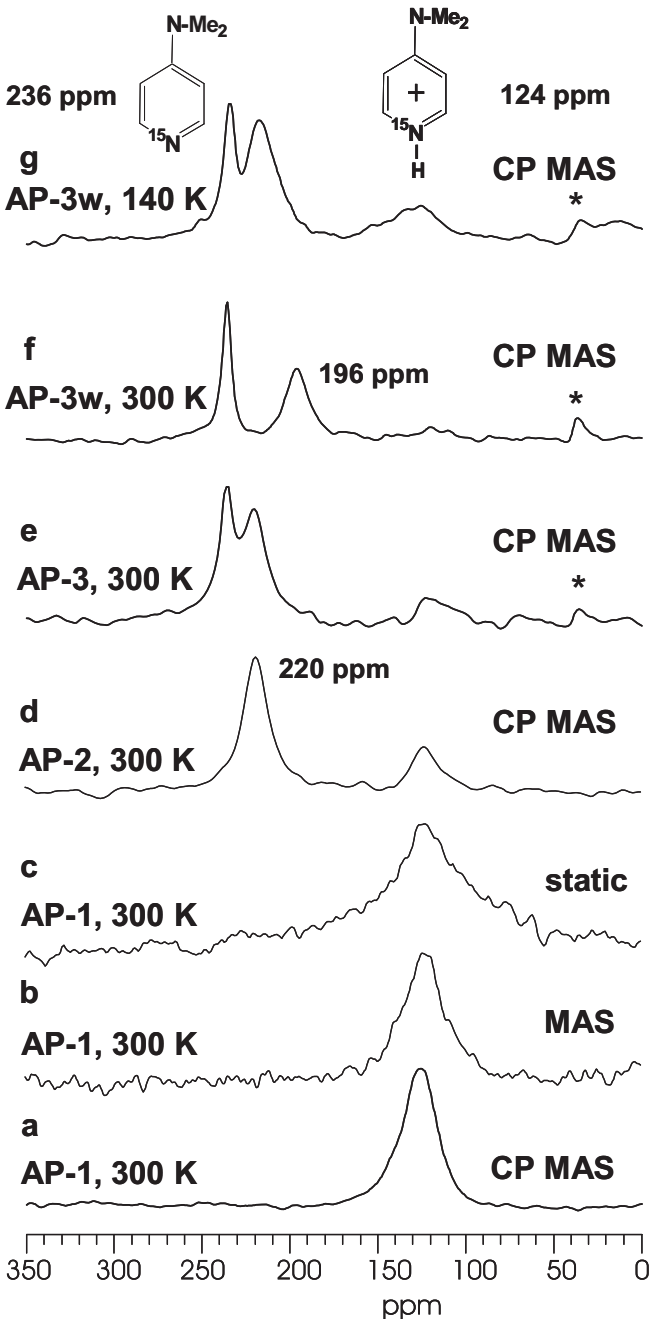

Fig. 1. ^{15}N NMR spectra of MCM-41 loaded with AP. Samples: (a) AP-1 at 300 K, CP MAS; (b) AP-1 at 300 K, MAS; (c) AP-1 at 300 K, CP static conditions; (d) AP-2 at 300 K, CP MAS; (e) AP-3 at 300 K, CP MAS; (f) AP-3w at 300 K, CP MAS; and (g) AP-3w at 140 K, CP MAS. Asterisks indicate spinning side bands.

signal at 236 ppm appear in the ^{15}N CPMAS NMR spectrum of AP-3, Fig. 1e. In order to explore the effect of the water content on the spectral features, sample AP-3w was prepared by adding 1 mg water to AP-3. The signal at 236 ppm is not affected by the presence of water. A new signal at 196 ppm appears instead of the signals at 216 and 124 ppm, Fig. 1f. In contrast, at 140 K the spectrum of AP-3w displays the same resonances as AP-3 at 300 K, Fig. 1g.

Fig. 2 presents ^{15}N NMR spectra of MCM-41 loaded with TBAP. Sample TBAP-1 contained about 0.2 TBAP molecules per nm^2 of the silica surface. MCM-41 material used for the preparation of this sample was stored in a desiccator over water. Spectra of TBAP-1 have been obtained under CPMAS conditions at 300 and 140 K

Author's personal copy

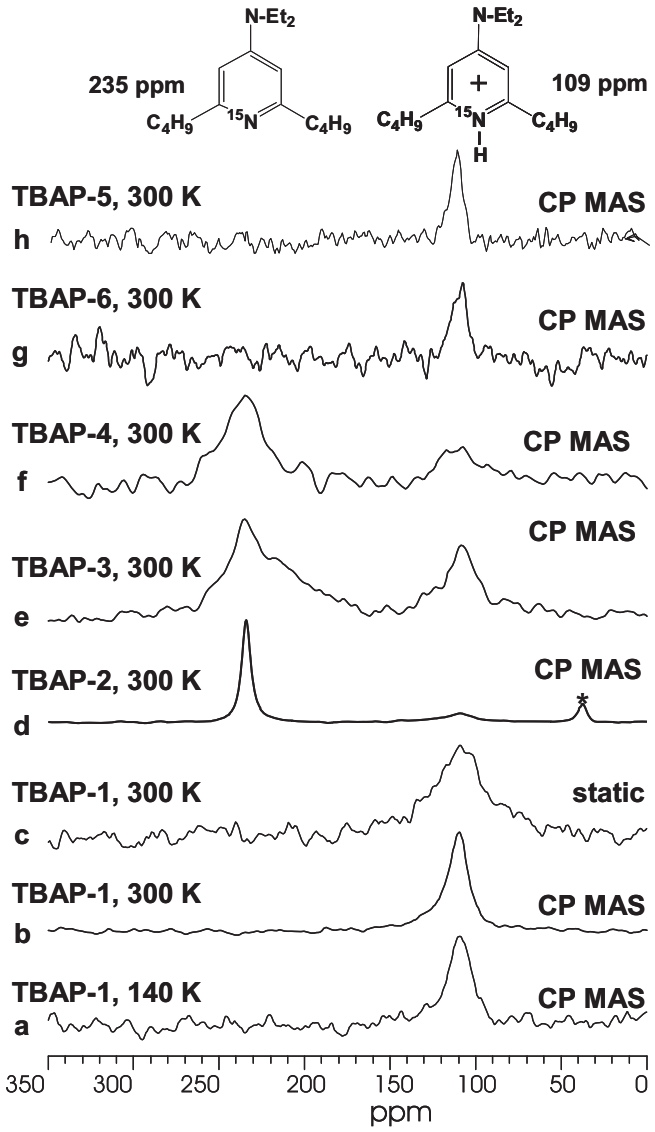

Fig. 2. ^{15}N NMR spectra of MCM-41 loaded with TBAP. Samples: (a) TBAP-1 at 140 K, CP MAS; (b) TBAP-1 at 300 K, CP MAS; (c) TBAP-1 at 300 K, CP static conditions; (d) TBAP-2 at 300 K, CP MAS; (e) TBAP-3 at 300 K, CP MAS; (f) TBAP-4 at 300 K, CP MAS; (g) TBAP-6 at 300 K, CP MAS; and (h) TBAP-5 at 300 K, CP MAS. Asterisks indicate spinning side bands.

and of a static sample at 300 K, Fig. 2a–c. A signal at 109 ppm is observed in all cases. The shape of the spectral line in the static spectrum is isotropic, Fig. 2c. Samples TBAP-2, TBAP-3 and TBAP-4 were prepared by introducing 2.5, 1.0 and 1.0 molecules per nm^2, respectively, into MCM-41 kept under ambient conditions, using CH_2Cl_2, C_6H_{14} or CH_3CN to assist the distribution of TBAP over the silica surface. In all cases, signals at 235 and 109 ppm are observed in the ^{15}N CPMAS NMR spectra, Fig. 2d–f. TBAP-5 and TBAP-6 were prepared using MCM-41 evacuated at 420 K. The samples were loaded with a small amount of TBAP. However, the preparation procedure did not allow to estimate quantitatively the number of the guest molecules per unit area of the surface. CH_2Cl_2 and C_6H_{14}, respectively, were used to assist the distribution of the base molecules in TBAP-5 and TBAP-6. In all cases, only the signal at 109 ppm is observed, Fig. 2g and h.

3.2. ^{1}H NMR

Fig. 3 shows ^{1}H MAS NMR spectra obtained at 300 and 140 K of MCM-41 evacuated at 420 K and the same material loaded with

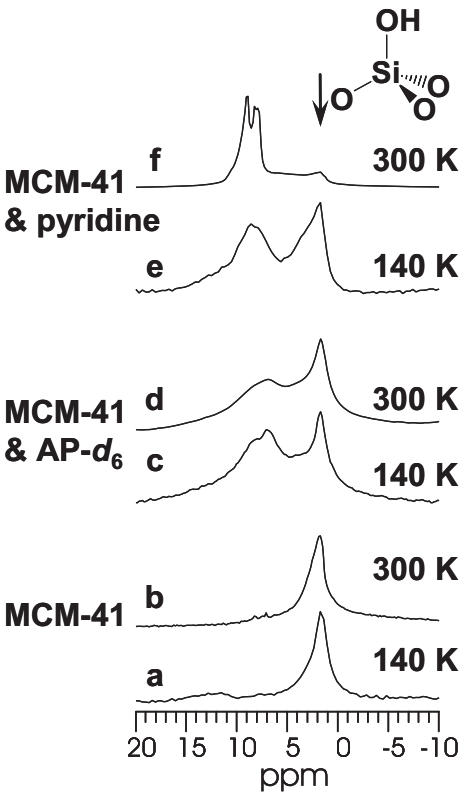

Fig. 3. ^{1}H MAS NMR spectra of dry MCM-41 at (a) 140 K and (b) 300 K, and of MCM-41 loaded with ½ monolayer of AP-d_6 at (c) 140 K and (d) 300 K, and of pyridine at (e) 140 K and (f) 300 K.

pyridine and AP-d_6. Deuteration of the methyl groups of AP was chosen to avoid signal overlapping. The mean surface density of the guests was 1.5 molecules per nm^2. In the absence of guest molecules MCM-41 exhibits a single resonance at 1.8 ppm, independent of temperature, Fig. 3a and b. The sample loaded with AP-d_6 shows additional signals at 9 ppm but again the spectra at 300 and 140 K are similar. In contrast, in the sample loaded with pyridine the resonance at 1.8 ppm is practically absent at 300 K although presents at 140 K, Fig. 3e and f.

4. Discussion

To provide an interpretation of the observed spectra, we need to review shortly what is known about the adsorption of pyridines in MCM-41 and the effect of hydrogen bonding on the spectral features of pyridine derivatives in ^{15}N NMR. Pyridine adsorbed into MCM-41 forms hydrogen-bonded complexes with surface silanol groups. While the isotropic ^{15}N chemical shift of hydrogen-bonded pyridine depends on the N···H distance [30], this interaction results in a high-field shift of 25 ppm relative to bulk pyridine [21]. A complete protonation should cause a high-field shift of about 125 ppm [30]. A value of 123 ppm was observed for a complex of $[TBAP\text{-}H]^+$ with $[BF_4]^-$ [33]. Protonation of di-tert-butylpyridine into acid zeolites results in high-field shifts between 124 and 129 ppm relative to bulk base [40]. At room temperature and a submonolayer loading, pyridine molecules jump rapidly between the hydrogen-bonded sites. Room temperature ^{15}N experiments on static samples of pyridine-^{15}N in MCM-41 at low coverage show a residual ^{15}N chemical shift anisotropy, indicating that the jumps of pyridine between different silanol groups is accompanied by an anisotropic reorientational diffusion. A quantitative analysis reveals that in this regime the rotation of pyridine around the molec-

Author's personal copy

ular C_2 axis is suppressed even at room temperature, and that the angle between the Si–O axes and the OH axes of silanol groups is about 47°. In the presence of excess of water, pyridine can form hydrogen-bonded complexes of different structures on silica surfaces, manifested by a broad set of peaks in low-temperature ^{15}N NMR spectra [21]. In the presence of excess of pyridine, 2:1 pyridine:water complexes will be formed. This interaction results in a high-field shift of 14 ppm relative to bulk pyridine [41]. Moreover, it is known that the density of the silanol groups on MCM-41 surface is about 3 per nm^2 [21]. Presumably, these groups are distributed uniformly on the surface and the distance between neighboring surface silanol groups is greater than 0.5 nm [42]. What is not yet understood is how pyridine can diffuse along the surface at room temperature without leaving it, when the distance between the silanol groups is so long.

4.1. Interaction of AP and TBAP with silanol groups of MCM-41

First we note the presence of an effective intramolecular cross-polarization (CP) between ^1H and ^{15}N spins in all studied samples. It indicates that the reorientation of adsorbed molecules is restricted at room temperature. The relative signal intensities in CP spectra depend on the dipolar ^{29}Si–^1H couplings. Nevertheless, it has been shown that the contact time of 5 ms is sufficient to measure correctly the relative signal intensities of different species which can be formed by pyridine adsorbed on silica surfaces [42]. The chemical shift anisotropy in the static spectra can be averaged out by a fast rotation of AP and TBAP around the molecular C_2 axis [21].

For AP-1, we observe the signal at 124 ppm that is shifted by 112 ppm to high-field as compared to bulk AP. This shift indicates that AP is involved in a hydrogen-bonded complex with proton transfer of the $[N{-}H]^+ \cdots O$ type. The $N \cdots H$ distance in this complex should be about 1.05 Å as can be estimated from the measured isotropic ^{15}N chemical shift of 112 ppm using a correlation reported in Ref. [30]. The surface density of these complexes is about 0.7 per nm^2. An increase of the surface density of adsorbed AP gives rise first to the appearance of the signal at 220 ppm, Fig. 1d, and finally to the signal at 236 ppm of bulk AP, Fig. 1e. Remember that the interaction of pyridine with the surface silanol groups shifts the resonance by 25 ppm to high-field as compared to bulk pyridine. AP is a stronger base than pyridine and its interaction with the surface silanol groups should result in a shorter hydrogen bond, that is a stronger high-field shift [30]. Accordingly, we conclude that the signal at 220 ppm cannot belong to a complex of AP with the surface silanol groups. MCM-41 used in this sample was kept at ambient conditions. Thus, it should contain some water and we ascribe this signal to a 2:1 AP:water complex. This prediction agrees with an increase of the ^{15}N chemical shift value from 14 ppm in the pyridine:water complex to 16 ppm in the AP:water complex as compared to bulk bases. The lengths of the $N \cdots H$ distances in the latter complex should be about 1.69 Å [41].

When water is added in excess (sample AP-3w), an exchange between the protonated and hydrogen-bonded AP species occurs at room temperature, Fig. 1f. This is concluded from the appearance of the signal at 196 ppm on account of the signals at 124 ppm (protonated AP) and 220 ppm (2:1 complex of AP with water). Bulk AP (signal at 236 ppm) remains excluded from this process, indicating that it is spatially separated from the adsorbed water. This finding probably indicates that the solvent-assisted adsorption does not prevent crystallization of the base outside the pore space when the molecules are excluded from the interaction with the surface or another adsorbed guest. At low temperature, the exchange is suppressed and the spectrum resembles the room temperature spectrum before the addition of water, Fig. 1g. The quality of the spectra is insufficient to analyze accurately the effect of excess of water on the integral intensities of the signals. It seems that in the presence of excess of water the integral intensity of the signal at 124 ppm increases slightly at the expense of the signal at 220 ppm. A simple line-shape analysis of the spectrum at 140 K suggests that there are about 0.8 $[AP\text{-}H]^+$ species per nm^2 in AP-3w. This indicates that although water assists the distribution of guest molecules along the surface, there is no clear correlation between the presence of water and the surface density of $[AP\text{-}H]^+$.

The tert-butyl groups in the ortho positions of TBAP prevent the formation of hydrogen-bonded complexes, excluding a full proton transfer to the base. Indeed, for TBAP-1, kept in a desiccator over water, we observe the signal at 109 ppm, which is shifted by 126 ppm to high-field as compared to bulk TBAP, Fig. 2. This value should correspond to practically free protonated $[TBAP\text{-}H]^+$ with a nitrogen-proton distance about 1.0 Å. In order to inspect the maximal amount of $[TBAP\text{-}H]^+$ species per unit area of MCM-41, we vary the amount of the adsorbed molecules and the solvent used to distribute TBAP along the surface, TBAP-2, TBAP-3 and TBAP-4. Irrespective of the amount of TBAP and the polarity of the solvent used, we observe a distribution between 0.2 and 0.3 $[TBAP\text{-}H]^+$ species per nm^2, Fig. 2d–f. The remaining loaded molecules forms bulk TBAP.

Thus, both AP and TBAP become protonated on the surface of MCM-41. The structures with proton transfer might be stabilized either by solvation with solvent that was used to distribute the guest along the surface, or by residual water, or because of interactions with neighboring silanol groups. The first possibility can be excluded since we observe almost the same amount of protonated species when the polar CH_3CN or the non-polar C_6H_{14} is used as the solvent, TBAP-4 and TBAP-3. The second possibility can also be excluded because no correlation between the amount of protonated species and the water content is observed. Furthermore, $[TBAP\text{-}H]^+$ is observed as well for samples prepared using MCM-41 evacuated at 420 K and water-free CH_2Cl_2 or C_6H_{14}, TBAP-5 and TBAP-6. Finally, if water were responsible for the stabilization of the species with proton transfer, one should expect a broad distribution of hydrogen bond geometries that is broad spectral lines, whereas in reality the line width of signals of the protonated and bulk species are very similar. Thus, the only feasible scenario to explain the presence of $[AP\text{-}H]^+$ and $[TBAP\text{-}H]^+$ species on the surface of MCM-41 is mutual interactions between silanol groups, as sketched in Figs. 4 and 5. In this case, however, the question arises why these silanol groups do not interact with each other in the absence of guests [21]. To answer this question, one needs to know the morphology of MCM-41 surface. Recently some of us discussed a possible surface pattern which agrees with available experimental data, but cannot be regarded as a confirmed model [21,42]. Here we sketch possible structural models, which may be experimentally inspected in later studies to prove or to reject them.

The simplest model is to assume a uniform distribution of silanol groups on the surface, Fig. 4. According to this model the next neighbors to any silanol group (Q^3 species) are silicate groups (Q^4 species), Fig. 4b, and the distance between neighboring silanol groups is between 0.5 and 0.6 nm. The "uniform" distribution model agrees with most available experimental data, viz., the density of surface silanol groups can be about 3 OH/nm^2, all groups can be functionalized [42], and the distance between the groups is too large for hydrogen bonds to form between them. What this model cannot explain is how pyridine diffuses along the surface at room temperature without leaving it [21]. Proton transfer to a guest requires the presence of hydrogen bonding between neighboring silanol groups. To be strong enough, these $O{-}H \cdots O^-$ hydrogen bonds should be nearly linear. Thus, in the framework of this model the proton transfer becomes possible only if the host–guest

Author's personal copy

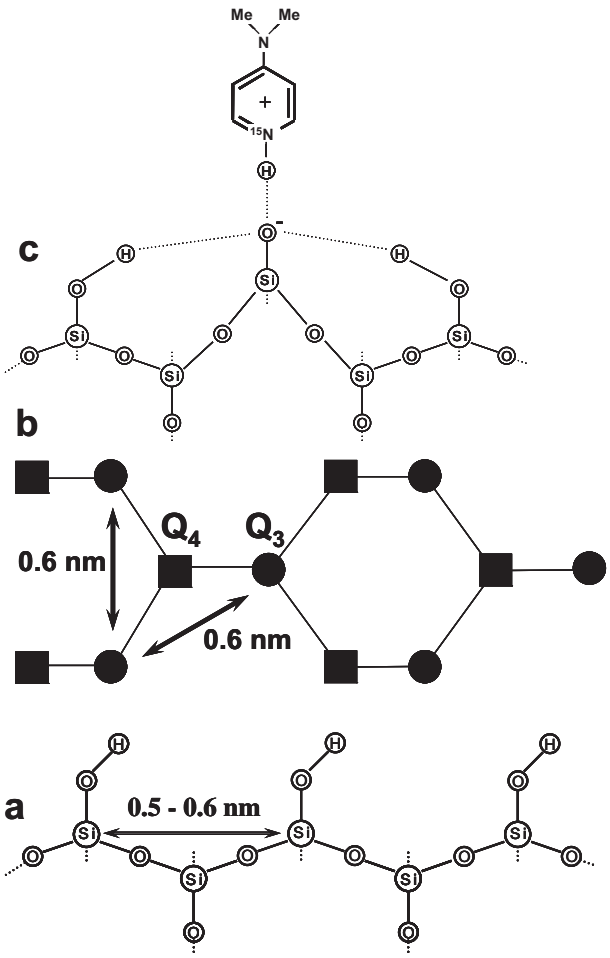

Fig. 4. Schematic representation of the "uniform" distribution model describing the distribution of silanol groups on inner surfaces of MCM-41 and the effect of proton transfer on the local structure. View along the surface (a) and normal to it (b), where rings stand for Q^3 species and squares stand for Q^4 species. The effect of proton transfer to AP (c) on the local structure of the surface.

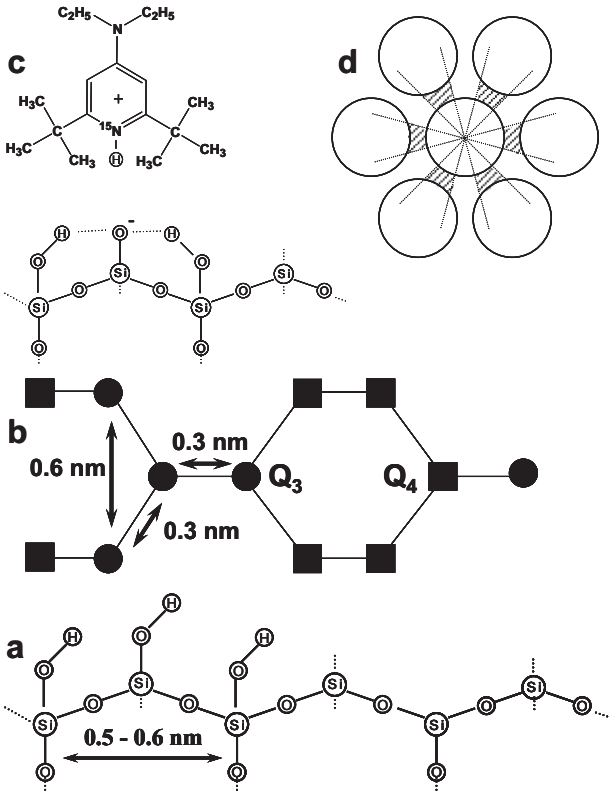

Fig. 5. Schematic representation of the "band" distribution model describing the distribution of silanol groups on inner surfaces of MCM-41 and the effect of proton transfer on the local structure. View along the surface (a) and normal to it (b), where rings stand for Q^3 species and squares stand for Q^4 species. The effect of proton transfer to TBAP (c) on the local structure of the surface. A sketch of the ordering of pores in a MCM-41 block (d).

interaction is strong enough to lift the deprotonating oxygen some distance up from the surface, Fig. 4c. Thus, in the "uniform" distribution model the proton transfer is accompanied by strong changes in the local surface structure, as illustrated for the AP protonation in Fig. 4c.

Alternatively, the observed behaviour can be explained by a model based on a non-uniform distribution of silanol groups. Such a non-uniform distribution may arise from the fact that the pore walls have a thickness less than 1 nm in the pore center-to-center direction, corresponding to roughly three silica species, and this confinement may lead to preferred structural motifs with a silanol density higher or lower than in regions of higher wall thickness. As sketched in Fig. 5d, there are six regions of low wall thickness per pore, forming "bands" along the pore axis. From the pore diameter (3.9 nm) we estimate that the width of the "band" is about 1 nm, roughly corresponding to three silica species. Thus, one may think of a surface made of alternating Q^3–Q^3–Q^3 and Q^4–Q^4–Q^4 "bands", Fig. 5a and b. According to this "band" model the distance between neighboring silanol groups in a band is about 0.3 nm. Since the mean density of surface silanol groups can still be about 3 OH/nm^2, this model can perfectly explain the surface diffusion of pyridine along pores at room temperature; with some constrains it is also possible that all silanol groups can be functionalized. In the framework of the "band" distribution model the mutual interactions between neighboring silanol groups responsible for the proton transfer to guests are obvious, since the groups are not in a plane. What is not clear is why the groups do not interact with each other in the absence of the guest. Moreover, the close spacing of silanol groups postulated in this model is in contradiction to the fact that di- and tripodical reagents like $(CH_3)_2Si(OH)_2$ and $CH_3Si(OH)_3$ can form only one covalent bond to the surface [42]. However, as in the "uniform" distribution model, one cannot exclude that the proton transfer is promoted by some change in the local surface structure, that makes the interaction between neighboring silanol groups possible. Protonation of TBAP in the framework of the "band" distribution model is illustrated in Fig. 5c. The current knowledge about the structure of the inner surfaces of MCM-41 is insufficient to decide which of the two models is more realistic than the other.

4.2. Dynamics of pyridine and AP on inner surfaces of MCM-41 at room temperature

As was already mentioned, the reorientation of AP and TBAP molecules, unlike pyridine, is strongly restricted at inner surfaces of MCM-41. In order to better understand this different behaviour it would be of interest to study in detail the surface diffusion of pyridine under conditions when the number of adsorbed molecules is smaller than the number of surface silanol groups. It was found that under this condition at room temperature pyridine molecules diffuse along the surface without leaving it [21]. The molecular mechanism of this diffusion is not clear, as it conflicts with the observation that the distance between neighboring surface silanol groups in MCM-41 is greater than 0.5 nm [42]. As a tentative model we propose that the inner surfaces of MCM-41 are not entirely

Author's personal copy

rigid so that strong interactions with guest molecules can affect the local structure of the pore walls. Such a non-rigid structure seems plausible in view of the small wall thickness of MCM-41. Since we have seen that $[AP\text{-}H]^+$ and $[TBAP\text{-}H]^+$ species are present even in water-free MCM-41, their stability can be explained exclusively as a result of mutual interactions between silanol groups. In order to corroborate this hypothesis we are at present studying the diffusion constants of pyridine in MCM-41. Results of this study will be reported elsewhere. Here we rely on a qualitative comparison the dynamics of pyridine and AP at these surfaces. The spectra shown in Fig. 3c–f were obtained with MCM-41 samples loaded with pyridine and AP in such a way that the number ratio of the surface silanol groups and the guest molecules is 2:1. At 300 K, pyridine molecules diffuse fast along the surface, making and breaking hydrogen bonds with silanol groups. The respective averaged signal should be located at about 6 ppm but can be broad and hidden in the base line, Fig. 3f. In contrast, at 140 K pyridine molecules are immobilized and the signal attributed to residual free silanol groups is observed at 1.8 ppm, Fig. 3e. For MCM-41 loaded with AP, the latter signal is present in spectra at both 140 and 300 K, Fig. 3c and d. This is a clear indication that protonated AP molecules remain localized at the deprotonated site of the surface. Remember that in the case of di-tert-butylpyridine adsorbed into acid zeolites protonated species were rigid on the surface, whereas non-protonated molecules were mobile [40].

5. Conclusions

The present work has shown that both 4-dimethylaminopyridine (AP) and 4-diethyl-2,6-di-tert-butylaminopyridine (TBAP) become protonated at the inner surface of MCM-41. The N···H distance in the $[AP\text{-}H]^+$ cation is lengthened to 1.05 Å due to hydrogen bonding to the surface. The N···H distance in the $[TBAP\text{-}H]^+$ cation is shorter and the interaction with the surface is purely electrostatic. Within experimental sensitivity of the present experiments, the surface density of protonated species is affected neither by the presence of water nor by the polarity of solvent used to distribute the bases along the surface. An analysis of the widths of the observed spectral lines indicates that water is not involved in or coordinated to the protonated species. We propose that strong electrostatic interactions can affect the local structure of the inner surfaces of MCM-41 such that neighboring silanol groups can interact with each other. Such local structures enable proton transfer to the guest and the formation of the $[AP\text{-}H]^+$ and $[TBAP\text{-}H]^+$ cations, as shown in Figs. 4 and 5. A maximal surface density of 0.8 protonated species per nm^2 has been observed for AP. While the mean surface density of the silanol groups is about 3 OH/nm^2 [21], we estimate that hydrogen bonding with two neighboring silanol groups is necessary to transfer the proton from a silanol group to AP. The maximal observed surface density of the $[TBAP\text{-}H]^+$ cations is only about 0.3 species per nm^2. Presumably, this reduction reflects constraints that the ortho tert-butyl groups impose to the proton transfer.

In contrast to pyridine, both $[AP\text{-}H]^+$ and $[TBAP\text{-}H]^+$ remain immobilized at the surface at room temperature, but are free to rotate around the molecular C_2 axis. In the presence of water and an excess of AP, 2:1 complexes can be formed, with water bonded between two bases. The N···H distance in this complex is about 1.69 Å. The reorientation of these complexes and molecular exchange between different species is slow at room temperature. At room temperature the presence of excess water facilitates an exchange of AP molecules bonded to water and protonated by the silanol groups. TBAP adsorbed on MCM-41 becomes either protonated by silanol groups or remains in a bulk phase. No indication for mobile TBAP molecules on the surface of MCM-41 has been found. TBAP does not interact with water adsorbed on the silica surface.

Acknowledgements

This work was supported by the Deutsche Forschungsgemeinschaft in the framework of SFB 448 "Mesoscopically Organized Composites" (Projects B1 and B2), the Russian Foundation of Basic Research (Project 08-03-00615), the Russian Ministry of Education and Science (Project RNP 2.1.1. 485), and the Federal Agency for Science and Innovation (Contract 02.740.11.0214).

References

[1] A. Corma, Chem. Rev. 95 (1995) 559–614.
[2] A. Taguchi, F. Schüth, Microporous Mesoporous Mater. 77 (2004) 1–45.
[3] G. Renard, M. Mureseanu, A. Galarneau, D.A. Lerner, D. Brunel, New J. Chem. 29 (2005) 912–918.
[4] D.J. Kim, B.C. Dunn, F. Huggins, G.P. Huffman, M. Kang, J.E. Yie, E.M. Eyring, Energy Fuels 20 (2006) 2608–2611.
[5] A. Galarneau, J. Iapichella, K. Bonhomme, F. Di Renzo, P. Kooyman, O. Terasaki, F. Fajula, Adv. Funct. Mater. 16 (2006) 1657–1667.
[6] D. Akcakayiran, D. Mauder, C. Hess, T.K. Sievers, D.G. Kurth, I.G. Shenderovich, H.-H. Limbach, G.H. Findenegg, J. Phys. Chem. B 112 (2008) 14637–14647.
[7] R.C. Hayward, P. Alberius-Henning, B.F. Chmelka, G.D. Stucky, Microporous Mesoporous Mater. 44 (2001) 619–624.
[8] R. Juarez, A. Padilla, A. Corma, H. Garcia, Catal. Commun. 10 (2009) 472–476.
[9] L. Gjerdaker, G.H. Soerland, D.W. Aksnes, Microporous Mesoporous Mater. 32 (1999) 305–310.
[10] F. Courivaud, E.W. Hansen, S. Kolboe, A. Karlsson, M. Stöcker, Microporous Mesoporous Mater. 37 (2000) 223–232.
[11] V. Ladizhansky, G. Hodes, S.J. Vega, Phys. Chem. B 104 (2000) 1939–1943.
[12] E. Gedat, A. Schreiber, J. Albrecht, I.G. Shenderovich, G.H. Findenegg, H.-H. Limbach, G. Buntkowsky, J. Phys. Chem. B 106 (2002) 1977–1984.
[13] L.T. Zhuravlev, Langmuir 3 (1987) 316–318.
[14] I.-S. Chuang, G.E. Maciel, J. Phys. Chem. B 101 (1997) 3052–3064.
[15] B. Ciavalleri, P. Ugliengo, J. Phys. Chem. B 104 (2000) 9491–9499.
[16] A. Corma, Chem. Rev. 97 (1997) 2373–2419.
[17] U. Ciesla, F. Schüth, Microporous Mesoporous Mater. 27 (1999) 131–149.
[18] E. Selli, L. Forni, Microporous Mesoporous Mater. 31 (1999) 129–140.
[19] J. Sauer, P. Ugliengo, E. Garrone, V.R. Saunders, Chem. Rev. 94 (1994) 2095–2160.
[20] J. Nawrocki, J. Chromatogr. A 779 (1997) 29–71.
[21] I.G. Shenderovich, G. Buntkowsky, A. Schreiber, E. Gedat, S. Sharif, J. Albrecht, N.S. Golubev, G.H. Findenegg, H.-H. Limbach, J. Phys. Chem. B 107 (2003) 11924–11939.
[22] K. Chapman, D. Crittenden, J. Bevitt, M.J.T. Jordan, J.E. Del Bene, J. Phys. Chem. 105 (2001) 5442–5449.
[23] J.E. Del Bene, M.J.T. Jordan, Mol. Struct. (THEOCHEM) 573 (2001) 11–23.
[24] F. Jiang, A. Kaltbeitzel, B. Fassbender, G. Brunklaus, H. Pu, W.H. Meyer, H.W. Spiess, G. Wegner, Macromol. Chem. Phys. 209 (2008) 2494–2503.
[25] R. Manriquez, F.A. Lopez-Dellamary, J. Frydel, Th. Emmler, H. Breitzke, G. Buntkowsky, H.-H. Limbach, I.G. Shenderovich, J. Phys. Chem. B 113 (2009) 934–940.
[26] D. Mauder, D. Akcakayiran, S.B. Lesnichin, G.H. Findenegg, I.G. Shenderovich, J. Phys. Chem. C 113 (2009) 19185–19192.
[27] B. Gruenberg, Th. Emmler, E. Gedat, I.G. Shenderovich, G.H. Findenegg, H.-H. Limbach, G. Buntkowsky, Chem. Eur. J. 10 (2004) 5689–5696.
[28] S. Pizzanelli, S. Kababya, V. Frydman, M. Landau, S. Vega, J. Phys. Chem. B 109 (2005) 8029–8039.
[29] G. Buntkowsky, H. Breitzke, A. Adamczyk, F. Roelofs, Th. Emmler, E. Gedat, B. Grünberg, Y. Xu, H.-H. Limbach, I.G. Shenderovich, A. Vyalikh, G.H. Findenegg, Phys. Chem. Chem. Phys. 9 (2007) 4843–4853.
[30] P. Lorente, I.G. Shenderovich, N.S. Golubev, G.S. Denisov, G. Buntkowsky, H.-H. Limbach, Magn. Reson. Chem. 39 (2001) S18–S29.
[31] http://www.cas.org/SCIFINDER/SCHOLAR/index.html.
[32] H.P. Hopkins, D.V. Jahagirdar, P.S. Moulik, D.H. Aue, H.M. Webb, W.R. Davidson, M.D. Pedleyt, J. Am. Chem. Soc. 106 (1984) 4341–4348.
[33] D.V. Andreeva, B. Ip, A. Gurinov, P.M. Tolstoy, I.G. Shenderovich, H.-H. Limbach, J. Phys. Chem. A 110 (2006) 10872–10879.
[34] M. Grün, K.K. Unger, A. Matsumoto, K. Tsutsumi, COPS IV (1997) 81–89.
[35] A. Schreiber, I. Ketelsen, G.H. Findenegg, Phys. Chem. Chem. Phys. 3 (2001) 1185–1195.
[36] P.I. Ravikovitch, A.V. Neimark, J. Phys. Chem. B 105 (2001) 6817–6823.
[37] M. Jaroinec, L.A. Solovyov, Langmuir 22 (2006) 6757–6760.
[38] M. Kumar, K. S. Singh, A. Agarwal, US Patent (2004) 0106801 A1.
[39] K.T. Potts, P.A. Winslow, Synthesis 9 (1987) 839–841.
[40] D. Farcasiu, R. Leu, A. Corma, J. Phys. Chem. B 106 (2002) 928–932.
[41] S. Sharif, I.G. Shenderovich, L. Gonzalez, G.S. Denisov, D.N. Silverman, H.-H. Limbach, J. Phys. Chem. A 111 (2007) 6084–6093.
[42] I.G. Shenderovich, D. Mauder, D. Akcakayiran, G. Buntkowsky, H.-H. Limbach, G.H. Findenegg, J. Phys. Chem. B 111 (2007) 12088–12096.